Accepted Manuscript

C-di-GMP turnover influences motility and biofilm formation in *Bacillus amyloliquefaciens* PG12

Yang Yang, Yan Li, Tantan Gao, Yue Zhang, Qi Wang

PII: S0923-2508(18)30065-2

DOI: 10.1016/j.resmic.2018.04.009

Reference: RESMIC 3655

To appear in: *Research in Microbiology*

Received Date: 10 December 2017

Revised Date: 22 March 2018

Accepted Date: 5 April 2018

Please cite this article as: Y. Yang, Y. Li, T. Gao, Y. Zhang, Q. Wang, C-di-GMP turnover influences motility and biofilm formation in *Bacillus amyloliquefaciens* PG12, *Research in Microbiologoy* (2018), doi: 10.1016/j.resmic.2018.04.009.

For publication

C-di-GMP turnover influences motility and biofilm formation in *Bacillus amyloliquefaciens* PG12

Yang Yang, Yan Li, Tantan Gao, Yue Zhang, Qi Wang*

Department of Plant Pathology, College of Plant Protection, China Agricultural University, Beijing 100193, China

*Corresponding author

Email addresses: wangqi@cau.edu.cn (Q. Wang), yybiocontrol@163.com (Y. Yang), liyancau@gmail.com (Y. Li), gaotantan0537@163.com (TT. Gao), yzhangvae@163.com (Y. Zhang).

Abstract

Bis-(3′→5′) cyclic dimeric guanosine monophosphate (c-di-GMP) is defined as a highly versatile secondary messenger in bacteria, coordinating diverse aspects of bacterial growth and behavior, including motility and biofilm formation. *Bacillus amyloliquefaciens* PG12 is an effective biocontrol agent against apple ring rot caused by *Botryosphaeria dothidea*. In this study, we characterized the core regulators of c-di-GMP turnover in *B. amyloliquefaciens* PG12. Using bioinformatic analysis, heterologous expression and biochemical characterization of knockout and overexpression derivatives, we identified and characterized two active diguanylate cyclases (which catalyze c-di-GMP biosynthesis), YhcK and YtrP and one active c-di-GMP phosphodiesterase (which degrades c-di-GMP), YuxH. Furthermore, we showed that elevating c-di-GMP levels up to a certain threshold inhibited the swimming motility of *B. amyloliquefaciens* PG12. Although *yhcK*, *ytrP* and *yuxH* knockout mutants did not display defects in biofilm formation, significant increases in c-di-GMP levels induced by YtrP or YuxH overexpression stimulated biofilm formation in *B. amyloliquefaciens* PG12. Our results indicate that *B. amyloliquefaciens* possesses a functional c-di-GMP signaling system that influences the bacterium's motility and ability to form biofilms. Since motility and biofilm formation influence the efficacy of biological control agent, our work provides a basis for engineering a more effective strain of *B. amyloliquefaciens* PG12.

Keywords: *Bacillus amyloliquefaciens*; Diguanylate cyclase; Gram-positive; Phosphodiesterase

1. Introduction

Bis-(3'→5') cyclic dimeric guanosine monophosphate (c-di-GMP) was first described as an allosteric activator of bacterial cellulose synthase in 1987 [1]. C-di-GMP is a small molecule produced from two molecules of GTP during a reaction catalyzed by diguanylate cyclases (DGCs) containing a GGDEF domain. Specific phosphodiesterases (PDEs) containing an EAL or HD-GYP domain catalyze the breakdown of c-di-GMP [2]. The number of GGDEF, EAL and HD-GYP domain-containing proteins varies greatly among bacteria. For instance, there is only one c-di-GMP-related protein in the Chlamydiae phylum, but over 7,000 across the Proteobacteria [3]. In the genus *Bacillus*, 59 c-di-GMP-related proteins have been predicted to exist in *B. selenitireducens* MLS10, whereas there are only two EAL or HD-GYP domain-containing proteins in *B. clausii* KSM-K16, implying that the c-di-GMP signaling pathway is not ubiquitous in *Bacillus* [4] (Fig. 1). This highly variable number of c-di-GMP-related proteins further suggests that there is variation in c-di-GMP networks. The c-di-GMP signaling pathway of *B. subtilis* NCIB3610, a model strain of the genus *Bacillus*, was first studied in 2012 [5] and was fully characterized in 2013 [6]. The *B. cereus* group, including several substantial clinical and financially important strains, were studied in 2016 [7]. Thus far, only *B. subtilis* and the *B. cereus* group have been shown to harbor a c-di-GMP signaling pathway in the *Bacillus* genus [5-7].

C-di-GMP has received increasing attention due to its involvement in motility transitions and biofilm formation [8-11]. To date, most of the research investigating c-di-GMP function had focused on Gram-negative species, especially pathogens such as *Pseudomonas aeruginosa*, *Klebsiella pneumonia*, *Vibrio cholerae* and *Yersinia pestis* [9, 12-17]. For example, in *P. aeruginosa*, it has been demonstrated that there is a correlation between a high

c-di-GMP concentration in the cell and biofilm formation, and between a low c-di-GMP level and motility [18]. In the biological control bacterium *P. protegens* Pf-5 [19], c-di-GMP signaling genes are influenced by two global regulators (GacA and RpoS) which also affect biological control activity [20]. However, motility and biofilm formation phenotypes of *gacA* and *rpoS* mutants are different [20-24]. Although c-di-GMP-regulated motility transitions in bacteria are closely related to biocontrol efficacy [25, 26], further studies are needed to understand the influence of c-di-GMP in biological control agents (BCAs). Since biofilm formation and motility critically influence colonization and thus determine the effectiveness of the biocontrol agent, research on c-di-GMP in BCAs may provide a basis for studying the relationship between the c-di-GMP pool and BCA capability.

B. amyloliquefaciens is a Gram-positive, aerobic and endospore-forming bacterium that exists in several environments, including soil, vegetation and animals [27]. Some *B. amyloliquefaciens* strains are important BCAs, since they are safe, ubiquitous and versatile, effectively protecting a wide range of plants from pathogen infection. Some *B. amyloliquefaciens* strains have been used commercially to promote plant growth and improve crop plant health [28]. For instance, *B. amyloliquefaciens* PG12, an effective BCA isolated from apple fruit, exhibits broad-spectrum antifungal activity by producing iturin A, which plays an important role in controlling apple ring rot disease [29]. Since undomesticated *B. amyloliquefaciens* strains are recalcitrant to genetic manipulation, it is unknown whether *B. amyloliquefaciens* posseses the c-di-GMP signaling system.

In this study, we predicted the existence of a c-di-GMP pathway in *B. amyloliquefaciens*

77 PG12 in silico and confirmed this prediction by heterologous expression in a c-di-GMP
78 riboswitch reporter and in a cellular c-di-GMP quantitative assay of c-di-GMP-related gene
79 knockout and overexpression mutants. Furthermore, we showed that increased c-di-GMP
80 levels reduced motility of the bacterium and enhanced the ability in biofilm formation.

81

2. Materials and methods

2.1. Bioinformatics

Open reading frames (ORFs) of genes containing GGDEF, EAL and HD-GYP domains were predicted using Prodigal (http://prodigal.ornl.gov/) with default parameters. The predicted amino acid sequences were searched against GenBank and clusters of orthologous group databases using BLASTP. The predicted, conserved active site was used as query in the Conserved Domain Database of the National Center for Biotechnology Information (NCBI, https://www.ncbi.nlm.nih.gov/cdd/).

2.2. Bacterial strains and growth conditions

Plasmids and strains used in this study were listed in Table 1. Primers are summarized in Table S1. *Escherichia coli* strain DH5α was used as a cloning host for plasmid construction. *E. coli* strain BL21 was used to overexpress putative DGCs. Plasmids were transformed into *B. amyloliquefaciens* strains after demethylation modification in *E. coli* strain EC135 [30]. *E. coli* DH5α and *B. amyloliquefaciens* strains were grown overnight at 37ºC on a rotary shaker (200 rpm) in Luria Bertani (LB) broth with necessary antibiotics. The concentrations of antibiotics used for *E. coli* strains were 100 μg/mL for ampicillin (Ap), 50 μg/mL for kanamycin (Km), 100 μg/mL for spectinomycin (Spec) and 40 μg/mL for zeocine. The concentrations of antibiotics used for *B. amyloliquefaciens* strains were 20 μg/mL for zeocine, 5 μg/mL for erythromycin (Erm) and 10 μg/mL for tetracycline (Tet).

2.3. Verification of putative DGCs using a c-di-GMP riboswitch-based dual fluorescence

reporter

C-di-GMP riboswitch reporters were constructed using methods described previously [31] and listed in Table 1. Briefly, ORFs of *ydaK*, *yhcK*, *ytrP* and *yybT* were amplified using *B. amyloliquefaciens* PG12 chromosomal DNA as template with primer pair ydaK-ORF-F/ydaK-ORF-R, yhcK-ORF-F/yhcK-ORF-R, ytrP-ORF-F/ytrP-ORF-R and yybT-ORF-F/yybT-ORF-R (primers listed in Table S1), followed by fusion (between *Nco*I and *Xho*I) into pET-28b(+), respectively. Subsequently, the constructed plasmids were co-transformed into *E. coli* BL21(DE3) with pRP0122-*Pbe-amcyan_Bc3-5_turborfp* to generate the strains used for putative DGC verification. The strain with pET-28b(+)-*pleD* was used as a positive control and pET-28b(+) was used as a negative control. BL21(DE3) strains were grown in LB containing 100 μg/mL Spec and 50 μg/mL Km medium at 28ºC and 200 rpm to an optical density (OD_{600}) of approximately 0.8. After adding IPTG at a final concentration of 1 mM, the cultures were incubated for 20 h under the same conditions and fluorescence color changes under bright field in response to intracellular c-di-GMP level. The cultures were concentrated about 10-fold and resuspended in water. They were later transferred to wells of 96-well microtiter plates for recording color intensity with a digital camera (Nikon, Japan). Then the samples were diluted to an OD_{600} of 0.1 with water. Fluorescence spectra of the samples were recorded with a SpectraMax® i3x Multi-Mode Detection Platform (Molecular Devices, USA).

2.4 Construction of knockout mutants and overexpression strains in B. amyloliquefaciens *PG12*

Putative c-di-GMP metabolic genes in PG12 were deleted as described [32] with slight modifications. Briefly, the *Bacillus-E. coli* shuttle vector pUBXC was transformed into *B. amyloliquefaciens* strains by electroporation [33]. The cells were grown at 37°C with shaking at 200 rpm until the OD_{600} reached about 0.5. Then, 1% (w/v) xylose was added. After 1 h incubation at 37°C with shaking at 170 rpm, 10 μL recombinant plasmid (Table 1) was mixed with 200 μL competent cells in a new 2 mL tube and incubated at 37°C with shaking at 120 rpm for another 2 h. Cells were plated on LB agar plates containing appropriate antibiotics. After PCR and DNA sequencing verification, the knockout mutants were cured of pUBXC by overnight culture in LB with or without 0.1% xylose and selected based on sensitivity to 20 μg/mL zeocine.

To construct overexpression strains of PG12, ORF of genes were amplified by PCR (primers listed in Table S1). The amplified products were cloned into the *Bacillus-E. coli* shuttle vector pUBX, which included an xyl operon that could be induced by xylose. The genes were expressed under control of the xyl promoter. The vectors for deleting c-di-GMP metabolic domain were produced by reverse PCR using pUBX-*ytrP* or pUBX-*yuxH* as template with primer pair ytrP-ko-F/ytrP-ko-R or yuxH-ko-F/yuxH-ko-R, respectively (primers listed in Table S1). After PCR and sequencing verification with primers pUBX-F/pUBX-R, the constructs were individually electroporated into knockout mutant backgrounds. Transformants were then selected on 5 μg/mL Erm or 10 μg/mL Tet and 20 μg/mL zeocine-containing LB plates and verified by PCR and DNA sequencing.

2.5. Bacterial growth rate analysis

Bacterial growth assays were performed using a microbiological growth analyzer (Labsystems, Finland). Overnight cultures were diluted 1:100 with LB. One hundred microliters of diluted culture was transferred to wells of 100-well plates (Fisher, USA). The plates were placed in a microbiological growth analyzer and incubated at 37°C for 12 h with continuous shaking. The OD_{600} of was measured every hour. Each sample had at least five replicates.

2.5.1. Quantification of intracellular c-di-GMP levels

B. amyloliquefaciens strains were cultured in LB medium at 37°C and 200 rpm, with appropriate antibiotics and 1% (w/v) xylose for strains containing the pUBX plasmid derivatives. At an OD_{600} of 0.8, the cells were precipitated (50 mL culture volume) by centrifugation at 4°C and c-di-GMP was extracted from the cell pellets immediately using a nucleotide extraction method reported previously [6] with slight modifications. Briefly, the cell pellet was resuspended in 1 mL ice-cold extraction solvent (a mixture of acetonitrile-methanol-water; 40:40:20 (v:v:v)) and incubated at 4°C for 15 min. The cell suspension was then heated to 95°C for 10 min. After cooling, the suspension was centrifuged at 14,000 rpm for 5 min. The extracted soluble molecules were then transferred to a new centrifuge tube and extraction from the remaining pellets was repeated twice with 500 μL extraction solvent at 4°C. The extraction volumes were combined for subsequent analysis. The combined extraction was identified and quantified by reversed-phase LC resolution prior to electrospray ionization tandem mass spectrometry (LC-MS/MS) as described previously [34], with slight modification. The experiment was performed using an Agilent 1290 (Agilent,

USA) liquid chromatograph equipped with a QQQ (Agilent 6460, USA) tandem mass spectrometer. A Synergi® Hydro-RP 2.0 mm×150 mm, 4 μm (Phenomenex) was used for LC separation, using a gradient elution of methanol as solvent A and 10 mM tributylamine and 15 mM glacial acetic acid diluted in water as solvent B. The gradient program was as follows: 0-1 min 2% A, 1-2 min 2% A to 20% A, 2-4 min 20% A to 65% A, 4-5 min 65% A to 95% A, 5-6 min 95% A, 6-6.1 min 95% A to 2% A, 6.1-10 min 2% A. The flow rate was set at 0.4 $mL \cdot min^{-1}$ and the injection volume was 10 μL. The total run time was 10 min for each sample. The negative ion mode was used to detect c-di-GMP. The mass spectrometer was operated in both electrospray ionization mode and in multiple-reaction monitoring mode. The nebulizer was set at 45 psi and the capillary was set at 4000 V. High-purity nitrogen served as both the nebulizing and dry gas. The gas temperature was held at 350ºC and the gas flow was 8 $L \cdot min^{-1}$. Chemically synthesized c-di-GMP (BIOLOG) was dissolved in the extraction buffer at concentrations of 1000, 500, 200, 100, 50, 25, 10, 5, 2.5, 1 and 0.5 ng/mL to generate a standard curve for calculating the c-di-GMP concentration in each extract.

2.6 Motility assay

Swimming motility was analyzed by inoculating 5 μL of an overnight culture in the center of a 0.3% LB agar plate as described previously [35]. For strains carrying the pUBX derivatives, 1% xylose was added to the medium. Plates were incubated at 37ºC until the surface of the inoculated plates had been covered by the fastest swimming cells. The diameter of the motility zone was measured. The assay was performed with three independent experiments, each with at least three technical replicates per strain.

186 *2.7. Biofilm formation assay*

187 The biofilm formation experiment was performed using a modified version of the
188 microtiter plate as described previously [36]. *B. amyloliquefaciens* strains were grown in LB
189 medium at 37°C overnight. Then, 200 μL of the dilutions from the overnight cultures with
190 fresh MSgg were transferred to wells of 96-well microtiter plates. For strains carrying the
191 pUBX derivatives, 1% xylose was added to the medium. The microtiter plates were incubated
192 statically at 37°C for about 48 h. The culture beneath the biofilm was drawn off carefully and
193 the biofilm in each well was washed with 200 μL sterile saline three times and fixed with
194 200 μL of 99 % (v/v) methanol for 15 min, followed by air-drying. The dried biofilms were
195 stained with 200 μL of 0.1 % crystal violet for 30 min. The microtiter plates were washed
196 again and dried at room temperature; then, 200 μL of 33% acetic acid were added to each well.
197 Absorbance at 570 nm of 50-fold dilutions was recorded using a SpectraMax® i3x
198 multi-mode detection platform. The assay was performed with three independent experiments
199 and each with eight technical replicates per strain tested.

3. Results

3.1. Genes predicted to be involved in c-di-GMP turnover in the undomesticated strain B. amyloliquefaciens *PG12*

To study the undomesticated strain *B. amyloliquefaciens* PG12 at the genetic level, we sequenced the genome using PacBio SMRT and obtained a complete sequence (unpublished data). We identified four ORFs encoding putative GGDEF domain proteins (*ydaK* [GenBank accession: MG674394], *yhcK* [GenBank accession: MG674395], *ytrP* [GenBank accession: MG674396] and *yybT* [GenBank accession: MG674397]) and two encoding EAL domain proteins (*ykuI* [GenBank accession: MG674398] and *yuxH* [GenBank accession: MG674399]) in the PG12 genome (Fig. 2). Conserved domain analysis (Fig S2) of the putative c-di-GMP metabolic enzymes in the NCBI Conserved Domains database (https://www.ncbi.nlm.nih.gov/Structure/cdd/wrpsb.cgi) showed that YdaK contained a GGDEF domain without an active site, which was required for DGC activity. YhcK harbored an intact GGDEF domain, and the transmembrane region of 5TMR-LYT. YtrP had an intact GGDEF domain and a GAF-like domain, which was a typical sensor domain that potentially binds to a wide range of ligands [37-39]. YybT shared 93% identity with the well-studied GdpP from *B. subtilis*, which was predicted to be a c-di-AMP phosphodiesterase, containing both a GGDEF-like and DHH family domains [40, 41]. YkuI comprised a degenerate EAL and YkuI_C domain; the latter was highly conserved in *Bacillus* genomes. YuxH contained EAL and HDOD domains (Fig. 2). Thus, only YhcK, YtrP and YuxH showed the potential for c-di-GMP metabolic enzyme activity.

3.2. YhcK and YtrP increased c-di-GMP levels in E. coli *strains*

To assess the c-di-GMP metabolic enzyme activity of putative GGDEF domain proteins, we fused ORFs of *ydaK*, *yhcK*, *ytrP* and *yybT* into pET-28b(+), respectively. The recombinant plasmid was then co-transformed into *E. coli* BL21 with pRP0122-*Pbe-amcyan_Bc3-5_turborfp*, which was found to exhibit detectable fluorescent color changes in response to increased intracellular c-di-GMP levels after induction of DGC [31]. *Bc3-5* is a native triple-tandem c-di-GMP riboswitch regulated by intracellular c-di-GMP levels. In the reporter, IPTG triggers expression of putative DGC. If the DGC is active, intracellular c-di-GMP accumulation activates the triple-tandem c-di-GMP riboswitch *Bc3-5* to turn on downstream *turborfp* transcription, generating red fluorescence emitted by TurboRFP. Conversely, if the putative DGC is "false", only AmCyan is expressed. Bc3-5/pleD was used as the positive control and Bc3-5/pET was used as the negative control (Table 1). PleD is a well-studied GGDEF domain containing protein from *Caulobacter crescentus* with high DGC activity [42].

The expression of putative DGCs was induced by adding IPTG to every sample of the final concentration of 1 mM in our test. Bc3-5/pET showed nearly constant green color from AmCyan fluorescence, with little interference from red TurboRFP fluorescence (Fig. 3A). The positive control Bc3-5/pleD exhibited a pink color, generated by a mix of TurboRFP and a few AmCyan proteins present within the cells (Fig. 3A). Bc3-5/ydaK and Bc3-5/yybT showed colors similar to Bc3-5/pET (Fig. 3A), demonstrating that YdaK and YybT had no c-di-GMP synthetic ability under such conditions. Bc3-5/yhcK and Bc3-5/ytrP exhibited a

bright orange and yellow color resulting from a mixture of TurboRFP and AmCyan proteins (Fig. 3A), demonstrating that they possessed genuine DGC activity in *E. coli*. The relative fluorescence intensity (RFI) was defined as the ratio between the fluorescence intensities of TurboRFP (574 nm) and AmCyan (489 nm). When we induced gene expression with identical doses of IPTG, this value increased in response to increasing DGC activity. Bc3-5/yhcK and Bc3-5/ytrP had remarkably higher RFI than Bc3-5/pET, while Bc3-5/ydaK and Bc3-5/yybT had an RFI similar to that of Bc3-5/pET (Fig. 3B). This result was consistent with conserved domain analysis. Moreover, it has been reported that the intracellular c-di-GMP level showed a linear correlation with RFI in the c-di-GMP riboswitch-based dual-fluorescence reporter [31]. We inferred that, in the heterologous expressing system, YhcK and YtrP had 72% and 23% activity of PleD, respectively. Since *yybT* was incapable of synthesizing c-di-GMP and exhibited ATP hydrolysis activity, as reported previously [40], we did not investigate it further. Based on these results, we believed that YhcK and YtrP were the only two functional DGCs in PG12.

3.3. YtrP and YuxH regulated c-di-GMP levels in vivo

To determine whether c-di-GMP was produced in vivo in *B. amyloliquefaciens*, we employed LC-MS/MS to detect the presence of c-di-GMP in *B. amyloliquefaciens* PG12 whole cell extracts. The average concentration of c-di-GMP in wild-type *B. amyloliquefaciens* PG12 was 61.4 pg/mL culture (Fig. 5A), suggesting that a c-di-GMP pathway might exist in *B. amyloliquefaciens* PG12. In contrast, wild-type *B. subtilis* has a concentration of 34.81 (± 2.30) ng of c-di-GMP per mg protein [43] and c-di-GMP level in *B. thuringiensis* 407

wild-type is out of the limit of detection, which is 0.8 ng/mL [7]. C-di-GMP level in *Xanthomonas oryzae* pv. *oryzicola* BLS256 is about 0.5 ng/mL [44], implying that the c-di-GMP levels in different strains fluctuate greatly.

To determine how genes involved in the c-di-GMP metabolic pathway influence levels of this secondary messenger in *B. amyloliquefaciens* PG12, we constructed a panel of deletion mutants for putative genes with c-di-GMP metabolic activity. The WT and deletion mutants showed similar growth curves, except for Δ*yhcK*, which grew significantly slower than the other strains, as assessed using Duncan's multiple range test (P <0.05) (Fig. 4). Surprisingly, the levels of c-di-GMP in Δ*yhcK* and Δ*ytrP* were similar to those in WT *B. amyloliquefaciens* PG12. It has been reported that the LC-MS/MS method was not accurate enough to detect differences in low levels of c-di-GMP [6, 7]. Here, we speculated that the actual c-di-GMP level of Δ*yhcK* and Δ*ytrP* may be lower than WT. In addition, the level of c-di-GMP in Δ*ykuI* was not significantly higher than that in the WT, indicating that YkuI did not degrade c-di-GMP. In contrast, c-di-GMP levels were much higher in Δ*yuxH* (3525.9 pg/mL) than in the WT (Fig. 5A; 61.4 pg/mL). Furthermore, when we overexpressed *yuxH* in the Δ*yuxH* mutant, c-di-GMP dropped to a level significantly lower than that observed in Δ*yuxH* with the empty pUBX vector or Δ*yuxH* with pUBX-*yuxH*$^{\Delta EAL}$ (Fig. 5C). This demonstrated that *yuxH* was the only PDE that reversibly regulates c-di-GMP in PG12.

Since we could not verify the function of YhcK and YtrP using knockout mutants, we switched to constructed overexpression strains. The growth curves of strains harboring pUBX with various inserts did not differ (Fig. S1). Overexpression of *ytrP* in Δ*ytrP* induced a sharp

increase in c-di-GMP levels compared with Δ*ytrP* (pUBX-*ytrP*$^{\Delta GGDEF}$), indicating that YtrP is a functional DGC (Fig. 5B). However, we were unable to transform pUBX-*yhcK* in Δ*yhcK* or in any other *B. amyloliquefaciens* PG12 derivative. To investigate the effect of high c-di-GMP levels, we also overexpressed *ytrP* in Δ*yuxH*. We found a sharp increase in c-di-GMP levels, from 3047.9 pg/mL in Δ*yuxH* with pUBX to 12686.4 pg/mL in Δ*yuxH* (pUBX-*ytrP*) with control of Δ*yuxH* with pUBX-*ytrP*$^{\Delta GGDEF}$ (Fig. 5C). Overall, *ytrP* increased c-di-GMP levels and *yuxH* decreased c-di-GMP levels in PG12 due to the active GGDEF or EAL domain.

3.4 C-di-GMP regulated the swimming motility of B. amyloliquefaciens *PG12*

Previous work in Gram-negative bacteria has shown that c-di-GMP signaling controls transitions between free-living and multicellular states [12]. To investigate the c-di-GMP effect on motility in *B. amyloliquefaciens* PG12, we assessed the swimming motility of knockout mutants for c-di-GMP metabolizing enzymes. The motility of Δ*yuxH* was reduced, while Δ*yhcK* and Δ*ytrP* showed a dramatic increase in motility compared with WT (Fig. 6A; 6B). The motility was reduced in strains with high c-di-GMP levels (Δ*yuxH*, Fig. 5A), and enhanced in strains with low levels of c-di-GMP (Δ*yhcK* or Δ*ytrP*). Thus, the c-di-GMP level exhibits an inverse effect on swimming motility.

To confirm this, we assessed the swimming motility of overexpression strains. Overexpression of *ytrP* (Δ*ytrP* (pUBX-*ytrP*)) significantly inhibited swimming motility; swimming motility was restored in Δ*ytrP* (pUBX-*ytrP*$^{\Delta GGDEF}$) with low c-di-GMP levels (Fig. 5B; 6C). Furthermore, overexpression of *yuxH* in Δ*yuxH* increased swimming motility to a

higher level compared with Δ*yuxH* (pUBX), WT (pUBX) and Δ*yuxH* (pUBX-*yuxH*$^{\Delta EAL}$) (Fig. 6C). The relationship between the swimming motility of overexpression strains and c-di-GMP level was consistent with the knockout mutants. However, the swimming motility of Δ*yuxH* (pUBX-*ytrP*), which had the highest c-di-GMP level (Fig. 5C), was not significantly weaker than that of Δ*yuxH* (pUBX) (Fig. 6C). In addition, strains with high concentrations of c-di-GMP (Δ*ytrP* with pUBX-*ytrP*, Δ*yuxH* with pUBX, Δ*yuxH* with pUBX- *yuxH*$^{\Delta EAL}$, Δ*yuxH* with pUBX-*ytrP* and Δ*yuxH* with pUBX-*ytrP*$^{\Delta GGDEF}$) showed no difference in motility (Fig. 5B; 5C; 6C). We speculated that in Δ*ytrP* (pUBX-*ytrP*), the intracellular concentration of c-di-GMP was high enough to inhibit swimming motility.

3.5 C-di-GMP functions in biofilm formation of B. amyloliquefaciens *PG12*

Since c-di-GMP signaling is also known to regulate biofilm formation, we next assessed biofilm formation of mutants with defects in c-di-GMP related genes in liquid biofilm-inducing medium (MSgg). Floating pellicle biofilms were visualized after 2 days of incubation at 37°C. Quantitative analysis of the biofilm biomass indicated that none of the mutants showed altered biofilm biomass compared to those formed by WT (Fig. 7A). When we augmented the c-di-GMP level by overexpression, the effects of increased c-di-GMP levels stimulated biofilm formation in Δ*yuxH* harboring pUBX compared with the WT harboring pUBX (Fig. 7B). Furthermore, Δ*yuxH* harboring pUBX-*ytrP*, which possessed the highest c-di-GMP level, developed the highest biofilm biomass, while Δ*yuxH* with pUBX-*yuxH* showed diminished biofilm formation (Fig. 7B). Moreover, the changes were restored in Δ*yuxH* (pUBX-*yuxH*$^{\Delta EAL}$) and Δ*yuxH* (pUBX-*ytrP*$^{\Delta GGDEF}$) (Fig. 7B). This

326 demonstrated that high c-di-GMP levels increased biofilm formation and that dramatic
327 changes in c-di-GMP levels were necessary to influence biofilm formation.

328

4. Discussion

The major findings of this study were that *B. amyloliquefaciens* PG12, a potential BCA, possessed a concise signaling system that regulated the production and degradation of c-di-GMP and influenced bacterial motility and biofilm formation. Since the c-di-GMP riboswitch reporter could only detect increased c-di-GMP levels, we were unable to test putative PDE activity using this system. Although the c-di-GMP levels rose significantly in *E. coli* after overexpression of *yhcK* and *ytrP*, we could not detect a significant decrease in c-di-GMP levels in Δ*yhcK* and Δ*ytrP* using LC-MS/MS, as the levels all fell outside the limit of quantification of the LC-MS/MS method. C-di-GMP levels were considerably elevated via the artificial expression of *ytrP* or deletion of *yuxH*, which indicated that *ytrP* was a DGC and *yuxH* was a c-di-GMP PDE in PG12. We were unable to overexpress *yhcK* in WT PG12 or any of the knockout mutants. Bioinformatic analysis and heterologous expression showed that YhcK had the potential to be a DGC. In addition, the swimming phenotype of Δ*yhcK* and Δ*ytrP* were alike, suggesting that YhcK was another DGC in PG12.

Elevated c-di-GMP levels in *B. amyloliquefaciens* PG12 increased biofilm formation and reduced motility, while lower c-di-GMP levels showed the opposite effect. In the *B. cereus* group, 13 predicted proteins containing putative c-di-GMP signaling domains are present and c-di-GMP signaling is linked to biofilm formation, motility and several other phenotypes important to the lifestyle of these bacteria [7]. In *B. subtilis*, three active DGCs, DgcP, DgcK and DgcW, and one active c-di-GMP phosphodiesterase, PdeH, have been characterized [5, 6]. By increasing the intracellular concentrations of c-di-GMP through overexpressing DgcP,

DgcK and DgcW or deleting PdeH, it was shown that increased c-di-GMP levels correlated with decreased motility, but did not influence biofilm formation [6]. Moreover, none of the mutants (including DGC knockout mutants) could increase motility [5, 6]. Biofilm formation is regulated by the effector protein YdaK, and expression of DGC genes is crucial for biofilm formation. They hypothesized that local and global c-di-GMP pools play important roles in signaling pathways [45, 46]. In our study, deleting YuxH also did not influence biofilm formation. However, highly fluctuating c-di-GMP levels induced by overexpression of DGC or PDE genes affected biofilm formation and, in *B. amyloliquefaciens* strains, biofilm formation was enhanced upon elevated intracellular c-di-GMP levels. Thus, our results offer direct evidence supporting their hypothesis.

In the NCBI database, the same c-di-GMP-related genes in *B. amyloliquefaciens* PG12 were predicted within 28 complete genomes of *B. amyloliquefaciens* strains. Homologous sequence alignment showed that the nucleotide sequences were conserved in most *B. amyloliquefaciens* strains (Table S2). The high level of nucleotide sequence similarity of the c-di-GMP genes in *B. amyloliquefaciens* strains suggested that the c-di-GMP signaling pathway was conserved. Several strains of *B. amyloliquefaciens* species are important BCAs [28, 29]. Members of this species are distinguished from domesticated model organisms by their ability to stimulate plant growth and suppress plant pathogens. Motility and biofilm formation are thought to be prerequisites for *B. amyloliquefaciens* strains colonizing surfaces [47]. Since colonization is a prerequisite for successful control of plant pathogens by BCAs, we speculated that the c-di-GMP signaling pathway influenced motility and biofilm formation, and may play an important role in engineering an effective strain. We plan to further study the

roles of *B. amyloliquefaciens* PG12 c-di-GMP in colonizing plants and controlling pathogens in future studies.

C-di-GMP binds to diverse classes of proteins and RNA-based receptors. The specific receptors sense changes in intracellular c-di-GMP and regulate important processes, including motility and biofilm formation [3]. Several classes of c-di-GMP receptors have been predicted to exist based on primary sequences, including PilZ domain receptors, I-site receptors, inactive EAL domain receptors, HD-GYP-like domain receptors, MshEN domain receptors and c-di-GMP riboswitches [48]. There are also less predictable c-di-GMP receptors. DgrA (YpfA), the only PilZ domain protein in *B. subtilis*, inhibits motility in response to rising levels of c-di-GMP [5, 6]. The corresponding orthologues of YdaK and YkuI in *B. subtilis* have been shown to exhibit no c-di-GMP metabolic activity [6]. However, YdaK carrying a degenerate GGDEF signature motif binds c-di-GMP with moderate affinity via the I-site (inhibition site in active DGCs) and regulates production of an unknown exopolysaccharide upon overproduction of the c-di-GMP synthetase DgcK [6, 45, 46]. In addition, a c-di-GMP riboswitch influences the adaptation and virulence of *B. thuringiensis* BMB171 by regulating transcription of collagen adhesion protein [49].

In this study, we identified proteins that directly regulate c-di-GMP turnover in *B. amyloliquefaciens*. We also discovered that c-di-GMP levels affect bacterial motility and biofilm formation in this strain. However, how this regulation works, what receptors are involved and what environmental or cellular signals are relevant remain to be explored.

Conflict of interest

The authors declare no conflict of interest.

Acknowledgements

We thank Prof. Ruifu Zhang (Nanjing Agricultural University) for generously providing the pUBXC plasmid and Prof. Jin He (Huazhong Agricultural University) for donating the c-di-GMP-riboswitch-based reporter. We also thank Yi Ding, Lili Li and Huawei Wang (Tsinghua University) for help with LC-MS/MS analysis. This work was supported by grants from the National Natural Science Foundation of China (No. 31672074) and the Beijing Municipal Natural Science Foundation (No.6172018).

References

[1] Ross P, Weinhouse H, Aloni Y, Michaeli D, Weinberger-Ohana P, Mayer R, et al. Regulation of cellulose synthesis in *Acetobacter xylinum* by cyclic diguanylic acid. Nature 1987;325:279-81.

[2] Schirmer T, Jenal U. Structural and mechanistic determinants of c-di-GMP signalling. Nat Rev Microbiol 2009;7:724-35.

[3] Romling U, Galperin MY, Gomelsky M. Cyclic di-GMP: the first 25 years of a universal bacterial second messenger. Microbiol Mol Biol R 2013;77:1-52.

[4] Chou S, Galperin MY. Diversity of cyclic di-GMP-binding proteins and mechanisms. J Bacteriol 2016;198:32-46.

[5] Chen Y, Chai YR, Gu JH, Losick R. Evidence for cyclic di-GMP-mediated signaling in

Bacillus subtilis. J Bacteriol 2012;194:5080-90.

[6] Gao XH, Mukherjee S, Matthews PM, Hammad LA, Kearns DB, Dann CE. Functional characterization of core components of the *Bacillus subtilis* cyclic-di-GMP signaling pathway. J Bacteriol 2013;195:4782-92.

[7] Fagerlund A, Smith V, Røhr ÅK, Lindbäck T, Parmer MP, Andersson KK, et al. Cyclic-di-GMP regulation of *Bacillus cereus* group biofilm formation. Mol Microbiol 2016;101(3):471-94.

[8] Jenal U, Reinders A, Lori C. Cyclic di-GMP: second messenger extraordinaire. Nat Rev Microbiol 2017;15:271.

[9] Valentini M, Filloux A. Biofilms and cyclic di-GMP (c-di-GMP) signaling: lessons from *Pseudomonas aeruginosa* and other bacteria. J Biol Chem 2016;291:12547-55.

[10] Romling U, Gomelsky M, Galperin MY. C-di-GMP: the dawning of a novel bacterial signalling system. Mol Microbiol 2005;57:629-39.

[11] Sadiq FA, Flint S, Li Y, Liu T, Lei Y, Sakandar HA, et al. New mechanistic insights into the motile-to-sessile switch in various bacteria with particular emphasis on *Bacillus subtilis* and *Pseudomonas aeruginosa*: a review. Biofouling 2017;33(4):306-26.

[12] McCarter LL, Gomelsky M. Fifty ways to inhibit motility via cyclic di-GMP: the emerging *Pseudomonas aeruginosa* swarming story. J Bacteriol 2015;197:406-09.

[13] McKee RW, Kariisa A, Mudrak B, Whitaker C, Tamayo R. A systematic analysis of the *in vitro* and *in vivo* functions of the HD-GYP domain proteins of *Vibrio cholerae*. Bmc Microbiol 2014;14:272.

[14] Jones CJ, Utada A, Davis KR, Thongsomboon W, Sanchez DZ, Banakar V, et al.

C-di-GMP regulates motile to sessile transition by modulating MshA pili biogenesis and near-surface motility behavior in *Vibrio cholerae*. Plos Pathog 2015;11:e1005068.

[15] Townsley L, Yildiz FH. Temperature affects c-di-GMP signalling and biofilm formation in *Vibrio cholerae*. Environ Microbiol 2015;17:4290-305.

[16] Schumacher MA, Zeng W. Structures of the activator of *K. pneumonia* biofilm formation, MrkH, indicates PilZ domains involved in c-di-GMP and DNA binding. Proceedings of the National Academy of Sciences of the United States of America 2016;113:10067-72.

[17] Ren G, Fan S, Guo X, Chen S, Sun Y. Differential regulation of c-di-GMP metabolic enzymes by environmental signals modulates biofilm formation in *Yersinia pestis*. Front Microbiol 2016;7:821

[18] Simm R, Morr M, Kader A, Nimtz M, Romling U. GGDEF and EAL domains inversely regulate cyclic di-GMP levels and transition from sessility to motility. Mol Microbiol 2004;53:1123-34.

[19] Ramette A, Frapolli M, Fischer-Le SM, Gruffaz C, Meyer JM, Defago G, et al. *Pseudomonas protegens* sp. nov., widespread plant-protecting bacteria producing the biocontrol compounds 2,4-diacetylphloroglucinol and pyoluteorin. Syst Appl Microbiol 2011;34:180-88.

[20] Kidarsa TA, Shaffer BT, Goebel NC, Roberts DP, Buyer JS, Johnson A, et al. Genes expressed by the biological control bacterium *Pseudomonas protegens* Pf-5 on seed surfaces under the control of the global regulators GacA and RpoS. Environ Microbiol 2013;15:716-35.

[21] Barahona E, Navazo A, Martinez-Granero F, Zea-Bonilla T, Perez-Jimenez RM, Martin

M, et al. *Pseudomonas fluorescens* F113 mutant with enhanced competitive colonization ability and improved biocontrol activity against fungal root pathogens. Appl Environ Microbiol 2011;77:5412-19.

[22] Matilla MA, Travieso ML, Ramos JL, Ramos-Gonzalez MI. Cyclic diguanylate turnover mediated by the sole GGDEF/EAL response regulator in *Pseudomonas putida*: its role in the rhizosphere and an analysis of its target processes. Environ Microbiol 2011;13:1745-66.

[23] Newell PD, Yoshioka S, Hvorecny KL, Monds RD, O'Toole GA. Systematic analysis of diguanylate cyclases that promote biofilm formation by *Pseudomonas fluorescens* Pf0-1. J Bacteriol 2011;193:4685-98.

[24] Hassan KA, Johnson A, Shaffer BT, Ren Q, Kidarsa TA, Elbourne LD, et al. Inactivation of the GacA response regulator in *Pseudomonas fluorescens* Pf-5 has far-reaching transcriptomic consequences. Environ Microbiol 2010;12:899-915.

[25] de Weert S, Vermeiren H, Mulders IH, Kuiper I, Hendrickx N, Bloemberg GV, et al. Flagella-driven chemotaxis towards exudate components is an important trait for tomato root colonization by *Pseudomonas fluorescens*. Mol Plant Microbe Interact 2002;15:1173-80.

[26] Vande BA, Lambrecht M, Vanderleyden J. Bacterial chemotactic motility is important for the initiation of wheat root colonization by *Azospirillum brasilense*. Microbiology 1998;144 (Pt 9):2599-606.

[27] Nicholson WL. Roles of *Bacillus* endospores in the environment. Cell Mol Life Sci 2002;59:410-16.

[28] Borriss R, Chen XH, Rueckert C, Blom J, Becker A, Baumgarth B, et al. Relationship of *Bacillus amyloliquefaciens* clades associated with strains DSM 7T and FZB42T: a proposal for *Bacillus amyloliquefaciens* subsp. *amyloliquefaciens* subsp. nov. and *Bacillus amyloliquefaciens* subsp. *plantarum* subsp. nov. based on complete genome sequence comparisons. Int J Syst Evol Microbiol 2011;61:1786-801.

[29] Chen X, Zhang Y, Fu X, Li Y, Wang Q. Isolation and characterization of *Bacillus amyloliquefaciens* PG12 for the biological control of apple ring rot. Postharvest Biol Tec 2016;115:113-21.

[30] Zhang G, Wang W, Deng A, Sun Z, Zhang Y, Liang Y, et al. A mimicking-of-DNA-methylation-patterns pipeline for overcoming the restriction barrier of bacteria. Plos Genet 2012;8:e1002987.

[31] Zhou H, Zheng C, Su JM, Chen B, Fu Y, Xie YQ, et al. Characterization of a natural triple-tandem c-di-GMP riboswitch and application of the riboswitch-based dual-fluorescence reporter. Sci Rep 2016;6:20871.

[32] Chen XT, Ji JB, Liu YC, Ye B, Zhou CY, Yan X. Artificial induction of genetic competence in *Bacillus amyloliquefaciens* isolates. Biotechnol Lett 2016;38:2109-17.

[33] Zhang G, Bao P, Zhang Y, Deng A, Chen N, Wen T. Enhancing electro-transformation competency of recalcitrant *Bacillus amyloliquefaciens* by combining cell-wall weakening and cell-membrane fluidity disturbing. Anal Biochem 2011;409:130-37.

[34] Bobrov AG, Kirillina O, Ryjenkov DA, Waters CM, Price PA, Fetherston JD, et al. Systematic analysis of cyclic di-GMP signalling enzymes and their role in biofilm formation and virulence in *Yersinia pestis*. Mol Microbiol 2011;79:533-51.

501 [35] Kearns DB. A field guide to bacterial swarming motility. Nat Rev Microbiol
502 2010;8:634-44.
503 [36] Hamon MA, Lazazzera BA. The sporulation transcription factor Spo0A is required for
504 biofilm development in *Bacillus subtilis*. Mol Microbiol 2001;42:1199-209.
505 [37] Biswas KH, Sopory S, Visweswariah SS. The GAF domain of the cGMP-binding,
506 cGMP-specific phosphodiesterase (PDE5) is a sensor and a sink for cGMP.
507 Biochemistry-Us 2008;47:3534-43.
508 [38] Savakis P, De Causmaecker S, Angerer V, Ruppert U, Anders K, Essen LO, et al.
509 Light-induced alteration of c-di-GMP level controls motility of *Synechocystis* sp. PCC
510 6803. Mol Microbiol 2012;85:239-51.
511 [39] Galperin MY. A census of membrane-bound and intracellular signal transduction proteins
512 in bacteria: bacterial IQ, extroverts and introverts. Bmc Microbiol 2005;5:1-19.
513 [40] Rao F, See RY, Zhang D, Toh DC, Ji Q, Liang Z. YybT is a signaling protein that
514 contains a cyclic dinucleotide phosphodiesterase domain and a GGDEF domain with
515 ATPase activity. J Biol Chem 2009;285:473-82.
516 [41] Luo Y, Helmann JD. Analysis of the role of *Bacillus subtilis* σM in β-lactam
517 resistance reveals an essential role for c-di-AMP in peptidoglycan homeostasis. Mol
518 Microbiol 2012;83:623-39.
519 [42] Aldridge P, Paul R, Goymer P, Rainey P, Jenal U. Role of the GGDEF regulator PleD in
520 polar development of *Caulobacter crescentus*. Mol Microbiol 2003;47:1695-708.
521 [43] Diethmaier C, Newman JA, Kovacs AT, Kaever V, Herzberg C, Rodrigues C, et al. The
522 YmdB phosphodiesterase is a global regulator of late adaptive responses in *Bacillus*

subtilis. J Bacteriol 2014;196:265-75.

[44] Wei C, Jiang W, Zhao M, Ling J, Zeng X, Deng J, et al. A systematic analysis of the role of GGDEF-EAL domain proteins in virulence and motility in *Xanthomonas oryzae* pv. *oryzicola*. Sci Rep 2016;6:23769.

[45] Bedrunka P, Graumann PL. Subcellular clustering of a putative c-di-GMP-dependent exopolysaccharide machinery affecting macro colony architecture in *Bacillus subtilis*. Env Microbiol Rep 2016;9:211-22.

[46] Bedrunka P, Graumann PL. New functions and subcellular localization patterns of c-di-GMP components (GGDEF domain proteins) in *B. subtilis*. Front Microbiol 2017;8:794.

[47] Dietel K, Beator B, Budiharjo A, Fan B, Borriss R. Bacterial traits involved in colonization of *Arabidopsis thaliana* roots by *Bacillus amyloliquefaciens* FZB42. Plant Pathology Journal 2013;29:59-66.

[48] Wang Y, Chin K, Tu Z, He J, Jones CJ, Sanchez DZ, et al. Nucleotide binding by the widespread high-affinity cyclic di-GMP receptor MshEN domain. Nat Commun 2016;7:12481.

[49] Tang Q, Kang Y, Qian H, Zhao Y, Wen W, Chou SH, et al. Cyclic di-GMP contributes to adaption and virulence of Bacillus thuringiensis through a riboswitch-regulated collagen adhesion protein. Sci Rep 2016;6:28807.

Fig. 1. A number of predicted c-di-GMP metabolic genes exist in various *Bacillus* species. According to "Distribution of GGDEF, EAL, HD-GYP and PilZ domains in bacterial genomes" (https://www.ncbi.nlm.nih.gov/Complete_Genomes/c-di-GMP.html), which predicts the numbers of c-di-GMP-related domains in representative complete genomes from all bacterial and archaeal species that were available in the NCBI's RefSeq database by the end of 2011, the number of c-di-GMP metabolic proteins in *Bacillus* species are highly variable [3]. The different domains are indicated using different colors: GGDEF (blue); GGDEF+EAL (orange); EAL (gray); HD-GYP (yellow). The source organisms are shown in the following order: *Bacillus weihenstephanensis* KBAB4 (GenBank accession: CP000903), *B. thuringiensis* serovar *konkukian* str. 97-27 (accession: AE017355), *B. subtilis* subsp. *subtilis* str. 168 (accession: AL009126), *B. selenitireducens* MLS10 (accession: NC_014219), *B. pumilus* SAFR-032 (accession: CP000813), *B. pseudofirmus* OF4 (accession: NC_013791), *B. megaterium* DSM 319 (accession: NC_014103), *B. licheniformis* ATCC 14580 (accession: AE017333), *B. halodurans* C-125 (accession: BA000004), *B. cytotoxicus* NVH 391-98 (accession: NC_009674), *B. coagulans* 2-6 (accession: NC_015634), *B. clausii* KSM-K16 (accession: AP006627), *B. cereus* ATCC 14579 (accession: AE016877), *B. cellulosilyticus* DSM 2522 (accession: NC_014829), *B. atrophaeus* 1942 (accession: NC_014639), *B. anthracis* str. Ames (accession: AE016879), *B. amyloliquefaciens* FZB42 (accession: CP000560).

Fig. 2. Genes predicted to be involved in c-di-GMP turnover in *B. amyloliquefaciens*. Schematic representation of c-di-GMP turnover domain structures in *B. amyloliquefaciens* PG12. Domain composition and organization of six putative c-di-GMP signaling proteins in *B.*

566 *amyloliquefaciens*, including four GGDEF domain proteins and two EAL domain proteins.
567 GGDEF domains are labelled in green, EAL domains are in red, degenerate GGDEF or EAL
568 domains are in dark green, TMs (transmembrane domains) are in orange and additional
569 domains predicted by Pfam are in gray. The annotations are as follows: 5TM-5TMR LYT,
570 transmembrane region of the 5TM-LYT (5-transmembrane receptors of the LytSYhcK type);
571 GAF-like, a superfamily represents the GAF domain and domains sharing protein structural
572 similarity; DDH and DHHA1, DHH subfamily members; YkuI-C, a highly conserved region
573 of the YkuI protein lies immediately downstream of the EAL; HDOD, HD/PDEase
574 superfamily.

575 **Fig. 3. Verification of heterogeneously expressed putative DGCs in *E. coli* BL21 (DE3)**
576 **using a *Bc3-5*-based dual-fluorescence c-di-GMP reporter.** The Bc3-5/pET and Bc3-5/pleD
577 strains were used as negative and positive controls, respectively. (A) Verification of putative
578 DGCs via a c-di-GMP reporter assay. Concentrated bacterial suspensions were photographed.
579 (B) Verification of putative DGCs via RFI measurements. Cultures were induced with IPTG
580 and RFI values were measured at 8 h post-induction. Error bars represented standard
581 deviation from three independent experiments, using one-way ANOVA (analysis of variance).
582 The letters (a–d) indicated significant differences (P <0.05) by Duncan's multiple range test.

583 **Fig. 4. Growth curve of WT PG12 and its derivatives.** The indicated strains were cultured
584 in LB medium and incubated at 37ºC for 12 h with continuous shaking. Five replicates were
585 performed for every strain. Uninoculated LB was used as a blank control. Error bars
586 represented standard deviation from three independent experiments, using one-way ANOVA.

587 **Fig. 5. Measurement of intracellular c-di-GMP levels in WT and knockout mutant**

588 **strains.** Assays were performed as described in Methods and concentration unit was pg/mL
589 culture. (A) The c-di-GMP concentrations were quantified in WT, Δ*ydaK*, Δ*yhcK*, Δ*ytrP*,
590 Δ*ykuI* and Δ*yuxH* mutants. (B) Quantification of c-di-GMP concentrations in WT with empty
591 plasmid (pUBX), Δ*ytrP* with pUBX, Δ*ytrP* with *ytrP* overexpression plasmid with/without
592 active GGDEF domain, respectively. (C) Quantification of c-di-GMP concentrations in the
593 WT with empty plasmid (pUBX) and Δ*yuxH* with pUBX, *yuxH* overexpression plasmid
594 with/without an active EAL domain, or *ytrP* overexpression plasmid with/without an active
595 GGDEF domain, respectively. Error bars represent standard deviation from three
596 independent experiments using one-way ANOVA. The letters (a–d) indicate significant
597 difference (P <0.05) by Duncan's multiple range test.

598 **Fig. 6. C-di-GMP levels regulate swimming motility.** (A) Swimming plates inoculated
599 with WT and the *yhcK*, *ytrP* and *yuxH* single knockout mutants. (B) Quantification of
600 swimming motility of various single mutants lacking the indicated putative c-di-GMP
601 signaling gene. (C) Quantification of swimming motility of bacteria in which *ytrP* and *yuxH*
602 were overexpressed. Strains with *ytrP* without active GGDEF domain overexpression plasmid
603 or *yuxH* without active EAL domain were used as controls. Error bars represented standard
604 deviation from three independent experiments, using one-way ANOVA. The letters (a–c)
605 indicated significant difference (P <0.05) by Duncan's multiple range test.

606 **Fig. 7. Biofilm formation was affected by the c-di-GMP level.** (A) Microtiter plate assay of
607 biofilm formation by PG12 and knockout mutants. (B) Microtiter plate assay of biofilm
608 formation by PG12 and Δ*yuxH* with pUBX plasmids. Error bars represent standard
609 deviation from three independent experiments using one-way ANOVA. The letters (a–e)

610 indicated significant difference (P <0.05) by Duncan's multiple range test.

611 **Fig. S1. Growth curves of PG12 derivatives.** The strains were cultured in LB with 1%
612 xylose and incubated at 37ºC for 12 h with continuous shaking. Five replicates were
613 performed for every strain. Uninoculated LB was used as a blank control. Error bars represent
614 standard deviation from three independent experiments, using one-way ANOVA.

615 **Fig. S2. Conserved domain analysis of the putative c-di-GMP metabolic enzymes.** The
616 amino acid sequences of putative c-di-GMP metabolic enzymes in PG12 were analyzed in the
617 NCBI Conserved Domains database (https://www.ncbi.nlm.nih.gov/Structure/cdd/wrpsb.cgi).

Table 1

Strains and plasmids used in this study.

Strain or plasmid	Relevant characteristics[a]	Reference or source
strains		
Escherichia coli		
DH5α	Cloning strain	Invitrogen
EC135	an *E. coli* strain lacking all the known endogenous Restriction-Modification systems and orphan MTases	[30]
BL21(DE3)	protein expression host	Beijing TransGen
Bc3-5/pET	BL21(DE3) containing pET-28b (+) and pRP0122-*Pbe-amcyan_Bc3-5_turb orfp*	[32]
Bc3-5/pleD	BL21(DE3) containing pET-28b (+)-*pleD* and	[32]

	pRP0122-*Pbe-amcyan_Bc3-5_turb* *orfp*	
Bc3-5/ydaK	BL21(DE3) containing pET-28b (+)-*ydaK* and pRP0122-*Pbe-amcyan_Bc3-5_turb* *orfp*	This study
Bc3-5/yhcK	BL21(DE3) containing pET-28b (+)-*yhcK* and pRP0122-*Pbe-amcyan_Bc3-5_turb* *orfp*	This study
Bc3-5/ytrP	BL21(DE3) containing pET-28b (+)-*ytrP* and pRP0122-*Pbe-amcyan_Bc3-5_turb* *orfp*	This study
Bc3-5/yybT	BL21(DE3) containing pET-28b (+)-*yybT* and pRP0122-*Pbe-amcyan_Bc3-5_turb* *orfp*	This study
Bacillus amyloliquefaciens		
WT	PG12 Wild type strain	[29]
Δ*ydaK*	PG12 Δ*ydaK*:: Erm^R	This study

Δ*yhcK*	PG12 Δ*yhcK*:: Erm^R	This study
Δ*ytrP*	PG12 Δ*ytrP*:: Erm^R	This study
Δ*ykuI*	PG12 ΔEAL_{ykuI}:: Tet^R	This study
Δ*yuxH*	PG12 Δ*yuxH*:: Tet^R	This study
plasmids		
pRP0122-P*be-amcyan_Bc3-5_turb orfp*	pRP0122 with triple-tandem riboswitch DNA in-between the *amcyan* and *turborfp* genes, $Spec^R$	[32]
pET-28b (+)	Empty vector, used as negative control, Km^R	Novagen
pET-28b (+)-*pleD*	Expression vector in *E. coli*; used as positive control, Km^R	[32]
pET-28b (+)-*ydaK*	Expression vector in *E. coli*; insert *ydaK* in MCS of pET-28b (+), Km^R	This study
pET-28b (+)-*yhcK*	Expression vector in *E. coli*; insert *yhcK* in MCS of pET-28b (+), Km^R	This study
pET-28b (+)-*ytrP*	Expression vector in *E. coli*; insert *ytrP* in MCS of pET-28b (+), Km^R	This study

pET-28b (+)-*yybT*	Expression vector in *E. coli*; insert *yybT* in MCS of pET-28b (+), Km^R	This study
pUBX	*Bacillus-Escherichia coli* shuttle vector containing P_{xylA}, *xylR*, t_0 transcription terminator, $Zeocine^R$	[33]
pUBXC	*Bacillus-Escherichia coli* shuttle vector pUBX containing $comK_{Bsu}$ under the control of xylose inducible system, $Zeocine^R$	[33]
pUBX-*ytrP*	*Bacillus-Escherichia coli* shuttle vector pUBX containing $ytrP_{PG12}$ under the control of xylose inducible system, $Zeocine^R$	This study
pUBX-$ytrP^{\Delta GGDEF}$	*Bacillus-Escherichia coli* shuttle vector pUBX-*ytrP* deleting conserved GGDEF domain, $Zeocine^R$	This study
pUBX-*yuxH*	*Bacillus-Escherichia coli* shuttle vector pUBX containing $yuxH_{PG12}$ under the control of xylose inducible system, $Zeocine^R$	This study
pUBX-$yuxH^{\Delta EAL}$	*Bacillus-Escherichia coli* shuttle	This

	vector pUBX-*yuxH* deleting	study
	conserved EAL domain, Zeocine^{R}	

[a] Erm^{R}, Tet^{R}, Spec^{R}, and Km^{R} stand for resistance to erythromycin, tetracycline, spectinomycin, and kanamycin, respectively.

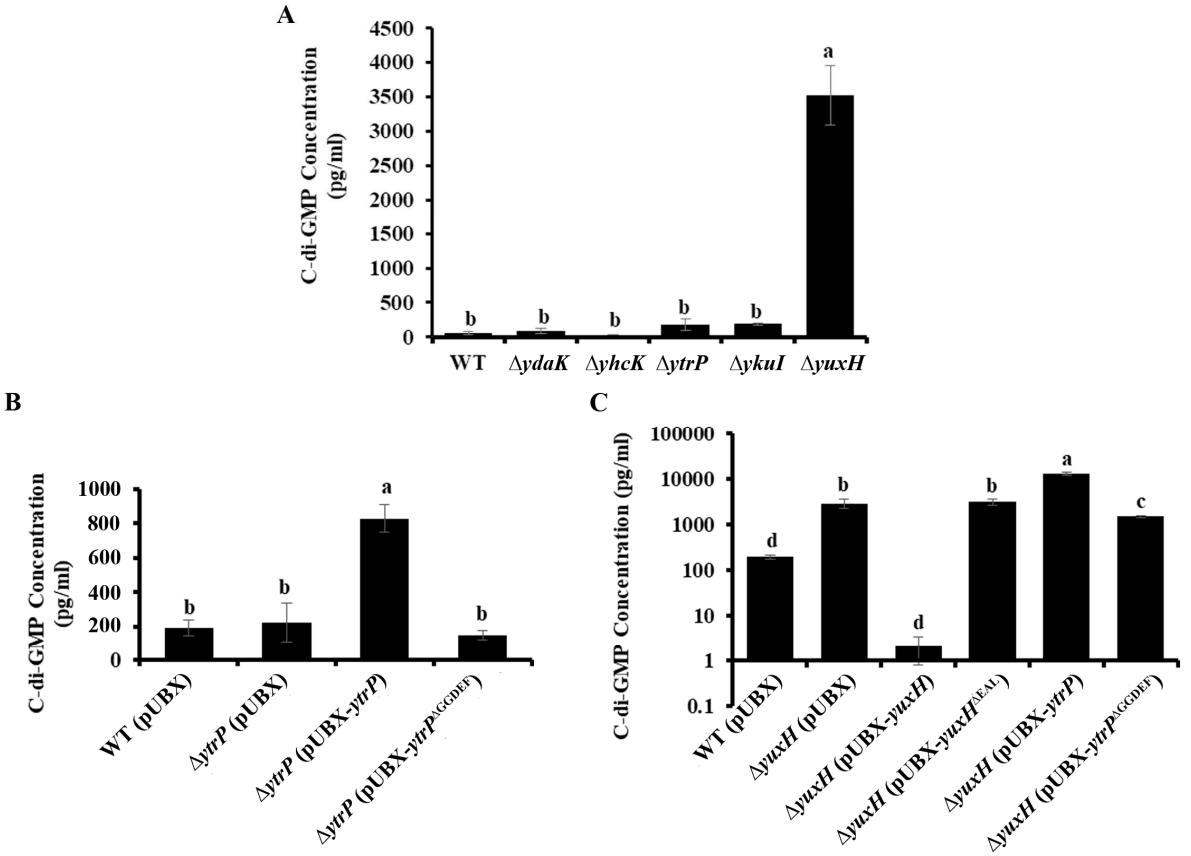

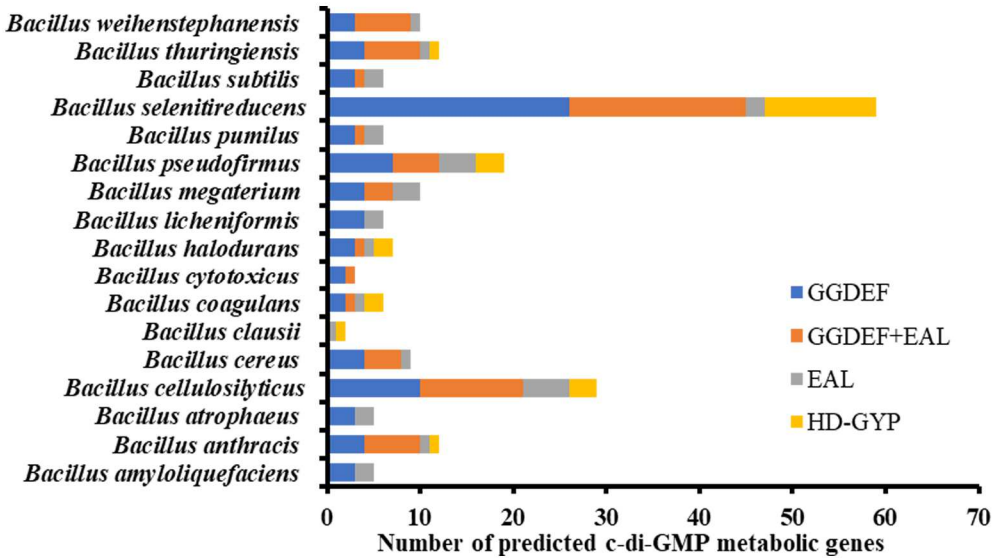

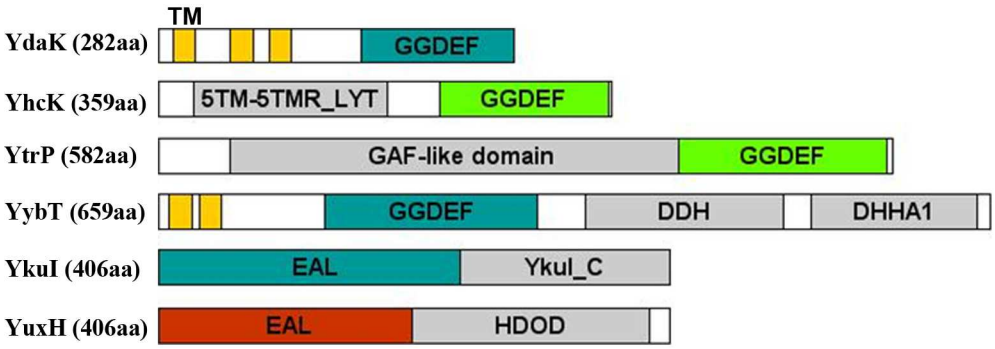

A

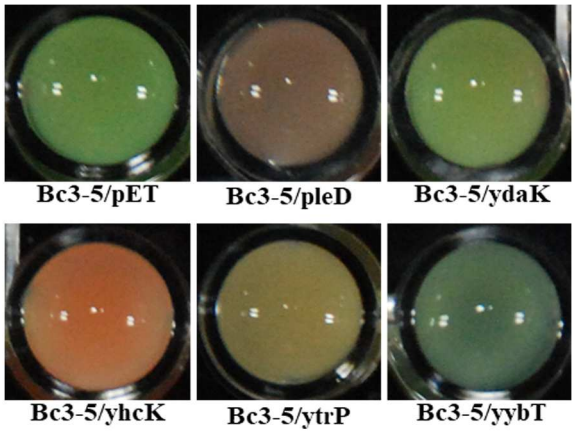

B

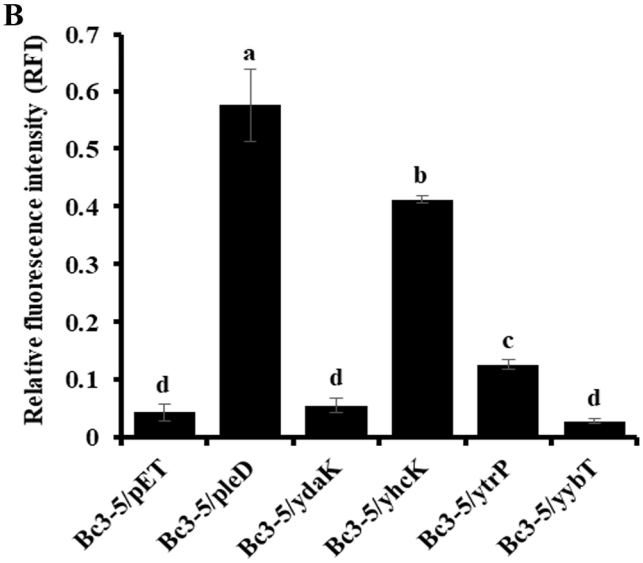

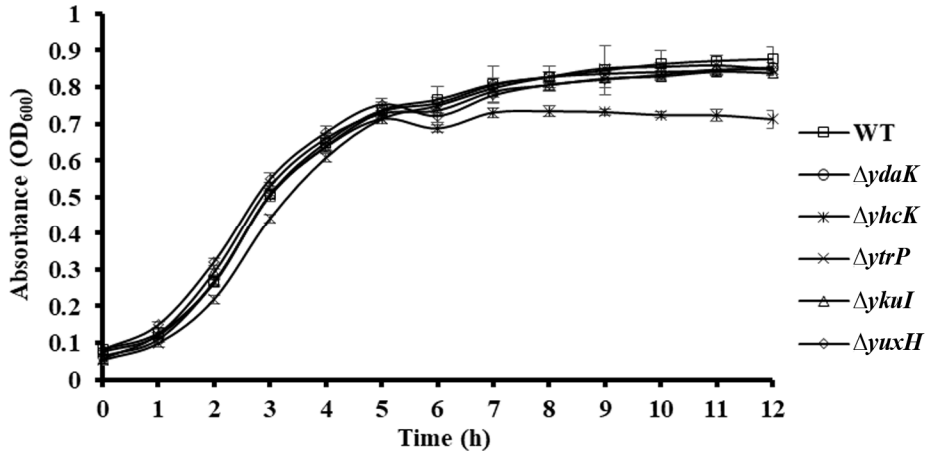

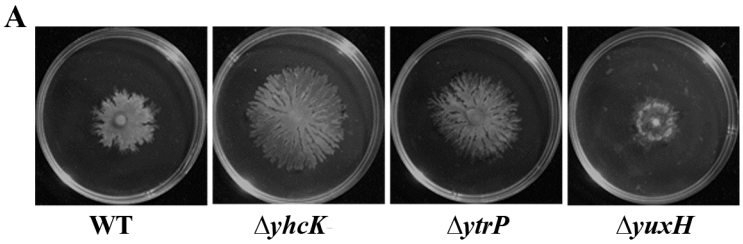
A
WT
ΔyhcK
ΔytrP
ΔyuxH

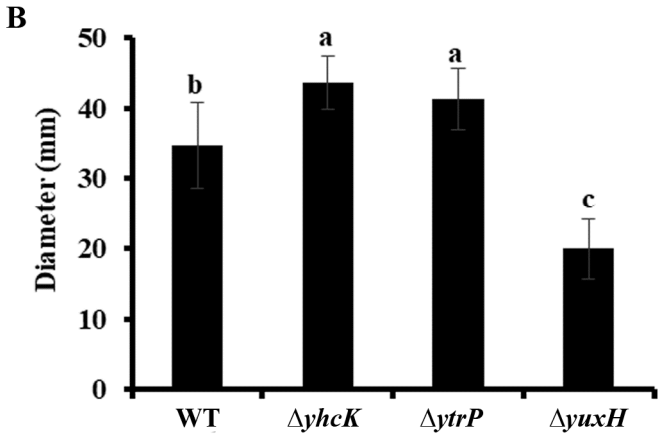
B
Diameter (mm)
50
40
30
20
10
0
b
a
a
c
WT
ΔyhcK
ΔytrP
ΔyuxH

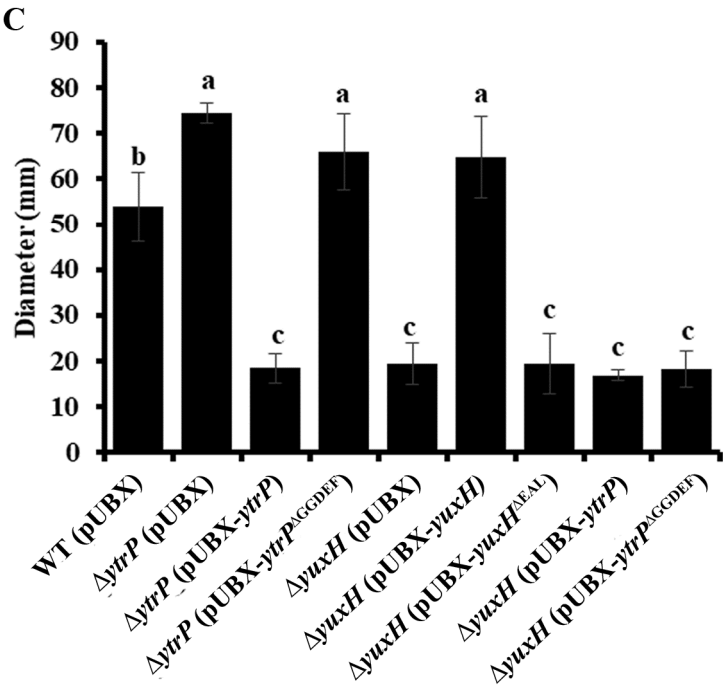
C
Diameter (mm)
90
80
70
60
50
40
30
20
10
0
b
a
c
a
c
a
c
c
c
WT (pUBX)
ΔytrP (pUBX)
ΔytrP (pUBX-ytrP)
ΔytrP (pUBX-ytrPAGGDEF)
ΔyuxH (pUBX)
ΔyuxH (pUBX-yuxH)
ΔyuxH (pUBX-yuxHAEAL)
ΔyuxH (pUBX-ytrP)
ΔyuxH (pUBX-ytrPAGGDEF)